

**LIDAR REMOTE SENSING DATA COLLECTION
BITTERROOT RIVER VALLEY, MONTANA**

AUGUST 20, 2008

Submitted to:
Laura Hendrix
215 S 4th Street, Suite F
Hamilton, MT 59840

Submitted by:

Watershed Sciences
215 SE 9th Ave., Ste. 106
Portland, OR 97214



LIDAR REMOTE SENSING DATA:

TABLE OF CONTENTS

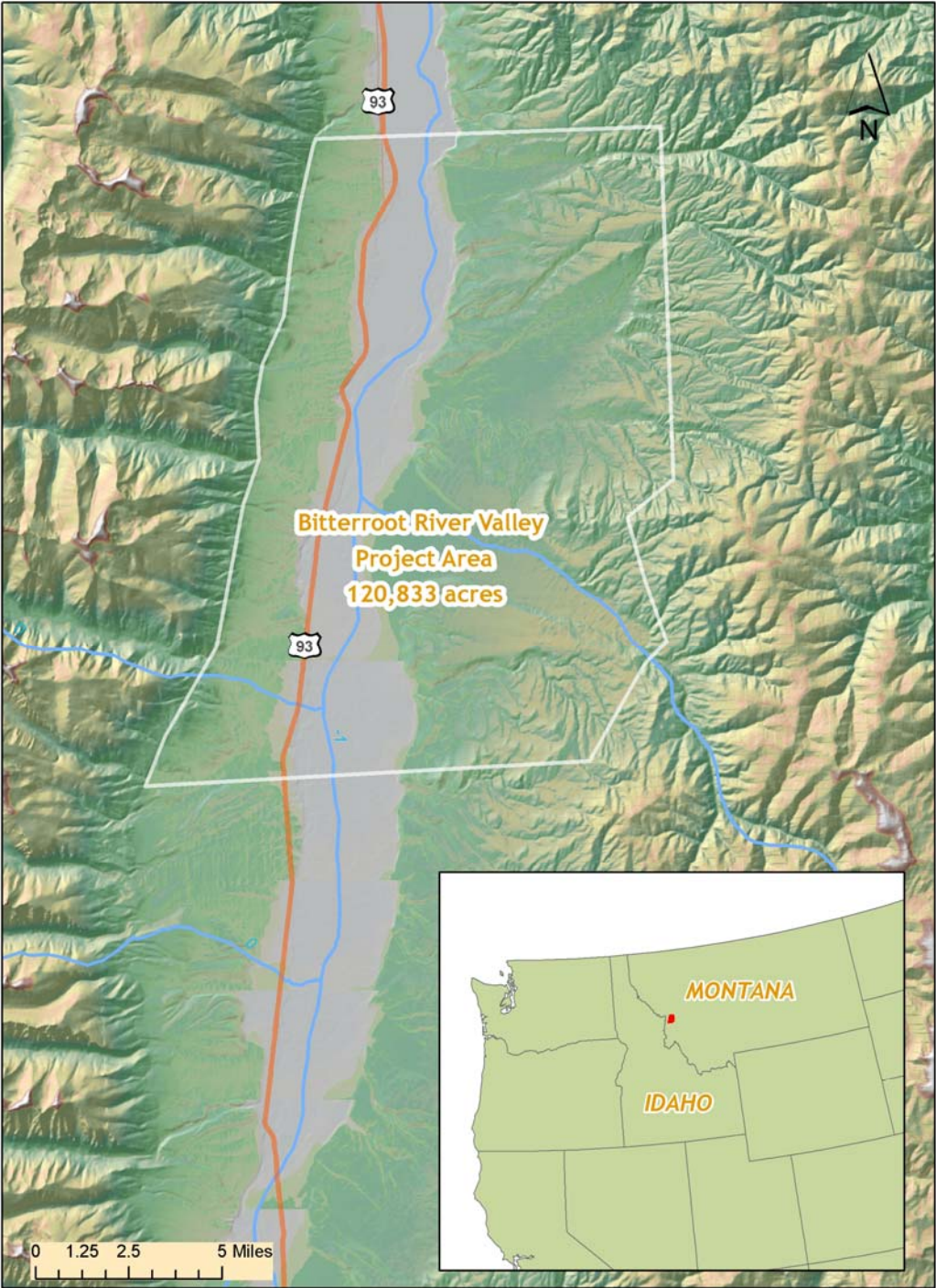
| | |
|--|-----------|
| 1. Overview | 1 |
| 1.1 Study Area | 1 |
| 1.2 Accuracy and Resolution..... | 2 |
| 1.3 Data Format, Projection, and Units | 2 |
| 2. Acquisition | 3 |
| 2.1 Airborne Survey Overview - Instrumentation and Methods | 3 |
| 2.2 LiDAR Acquisition | 4 |
| 2.3 Ground Survey - Instrumentation and Methods | 5 |
| 3. LiDAR Data Processing | 7 |
| 3.1 Applications and Work Flow Overview | 7 |
| 3.2 Aircraft Kinematic GPS and IMU Data..... | 7 |
| 3.3 Laser Point Processing | 8 |
| 3.4 Contour Development | 9 |
| 4. LiDAR Accuracy and Resolution | 10 |
| 4.1 Laser Point Accuracy | 10 |
| 4.1.1 Relative Accuracy..... | 10 |
| 4.1.2 Absolute Accuracy | 13 |
| 4.2 Accuracy per Land Cover | 14 |
| 4.3 Data Density/Resolution | 15 |
| 4.3.1 First Return Laser Pulses per Square Meter | 15 |
| 4.3.2 Ground Classified Points per Square Meter | 17 |
| 5. Data Specifications | 19 |
| 6. Projection/Datum and Units | 19 |
| 7. Deliverables | 19 |
| 7.1 Point Data..... | 19 |
| 7.2 Raster Data | 19 |
| 7.3 Vector Data | 19 |
| 7.4 Data Report | 19 |
| 8. Selected Images | 20 |
| 9. Glossary | 24 |
| 10. Citations | 25 |

1. Overview

1.1 Study Area

Watershed Sciences, Inc. collected Light Detection and Ranging data (LiDAR) of the Bitterroot River Valley on June 1-3 and 5 -6, 2008. The requested LiDAR area of interest (AOI) totals approximately 185 square miles, or 118,730 acres. This area was buffered by 100 meters to ensure data coverage, resulting in a total area flown (TAF) of 120,833 acres.

Figure 1.1. Bitterroot River Valley study area, Montana.



1.2 Accuracy and Resolution

Real time kinematic surveys (RTK) were conducted across multiple flightlines in the study area as quality assurance. The accuracy of the LiDAR data is described as standard deviations of divergence (σ) from RTK ground survey points and root mean square error (RMSE), which measures bias upward or downward. The data have the following accuracy statistics:

- RMSE of 0.02 meters
- 1-sigma absolute deviation of 0.02 meters
- 2-sigma absolute deviation of 0.04 meters

Data resolution specifications are for ≥ 6 points per square meter. Total average pulse density for the Bitterroot River valley study areas is 6 points per square meter.

1.3 Data Format, Projection, and Units

Projection: Montana State Plane FIPS 2500; Vertical datum: NAVD88/Geoid03;
Horizontal datum: NAD83
Units: Meters
Delineation: Processing bins

Deliverables include:

- Report of data collection methods and summary statistics
- 1-meter resolution bare-earth digital elevation model in ESRI grid format
- 1-meter resolution highest-hit digital elevation model in ESRI grid format
- ½-meter resolution intensity images in GeoTIFF format conforming to 750-meter processing tiles
- 2-foot contour data in .dwg and .shp formats conforming to 750-meter processing tiles
- 3-foot resolution ground density raster (corresponding to contour uncertainty information)
- All return points in Las v.1.1 format

2. Acquisition

2.1 Airborne Survey Overview - Instrumentation and Methods

The LiDAR survey utilized a Leica ALS50 Phase II sensor mounted in Cessna Caravan 208B. The Leica ALS50 Phase II system was set to acquire $\geq 105,000$ laser pulses per second (i.e. 105 kHz pulse rate) and flown at 1000 meters above ground level (AGL), capturing a scan angle of $\pm 14^\circ$ from nadir¹ (see Table 2.1). These settings are developed to yield points with an average native pulse density of ≥ 6 points per square meter over terrestrial surfaces. Some types of surfaces (i.e., dense vegetation or water) may return fewer pulses than the laser originally emitted. Therefore, the delivered density can be less than the native density and vary according to distributions of terrain, land cover, and water bodies.



The Cessna Caravan is a powerful and stable platform, ideal for the mountainous terrain of the Pacific Northwest. The Leica ALS50 sensor head installed in the Caravan is shown on the right.

The completed area was surveyed with opposing flight line side-lap of $\geq 50\%$ ($\geq 100\%$ overlap) to reduce laser shadowing and increase surface laser painting. The system allows up to four range measurements per pulse, and all discernable laser returns were processed for the output dataset.

To solve for laser point position, an accurate description of aircraft position and attitude is vital. Aircraft position is described as x, y, and z and measured twice per second (2 Hz) by an onboard differential GPS unit. Aircraft attitude is measured 200 times per second (200 Hz) as pitch, roll, and yaw (heading) from an onboard inertial measurement unit (IMU).

Table 2.1 LiDAR Survey Specifications

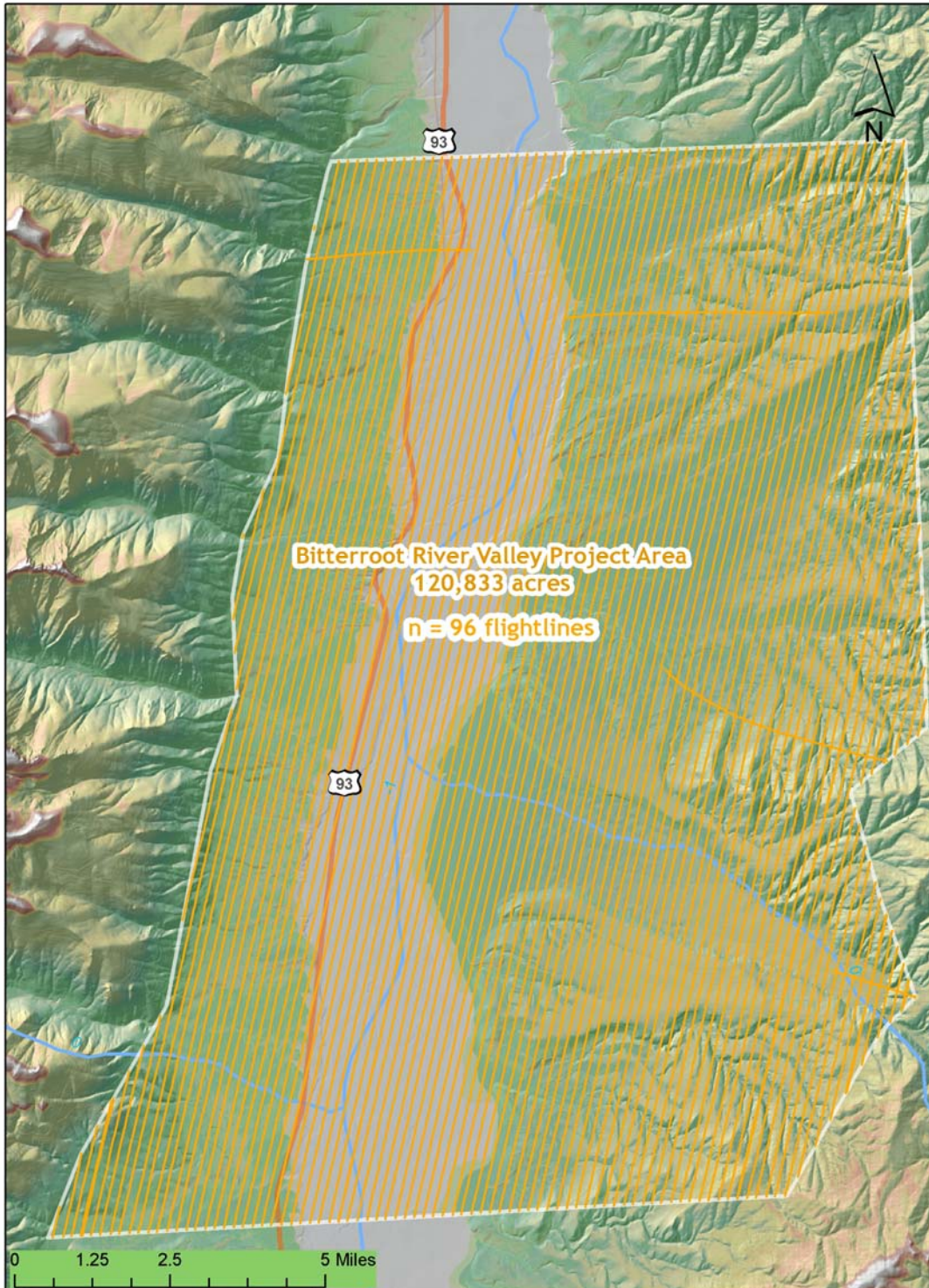
| | |
|------------------------------|---|
| Sensor | Leica ALS50 Phase II |
| Survey Altitude (AGL) | 1000 m |
| Pulse Rate | >105 kHz |
| Pulse Mode | Single |
| Mirror Scan Rate | 52.2 Hz |
| Field of View | 28° ($\pm 14^\circ$ from nadir) |
| Roll Compensated | Up to 20° |
| Overlap | 100% (50% Side-lap) |

¹ Nadir refers to a vector perpendicular to the ground directly below the aircraft. Nadir is commonly used to measure the angle from the vector and is referred to as “degrees from nadir”.

2.2 LiDAR Acquisition

LiDAR data was collected at the Bitterroot River Valley study area on June 1-3, 5, and 6, 2008. The flightlines conducted are shown in Figure 2.1.

Figure 2.1. Flightlines over the Bitterroot River Valley area.



2.3 Ground Survey - Instrumentation and Methods

During the LiDAR survey, static (1 Hz recording frequency) ground surveys were conducted over monuments with known coordinates. Monument coordinates are provided in **Table 2.2** and shown in **Figure 2.2**. After the airborne survey, the static GPS data are processed using triangulation with CORS stations and checked against the Online Positioning User Service (OPUS²) to quantify daily variance. Multiple sessions are processed over the same monument to confirm antenna height measurements and reported position accuracy.

The coordinates used were certified by a licensed surveyor (George Marshall PLS) and the coordinates used are accurate to within 0.01 meters.

Table 2.2. Base Station Surveyed Coordinates, (NAD83/NAVD88, OPUS corrected) used for kinematic post-processing of the aircraft GPS data for the Bitterroot River Valley study area.

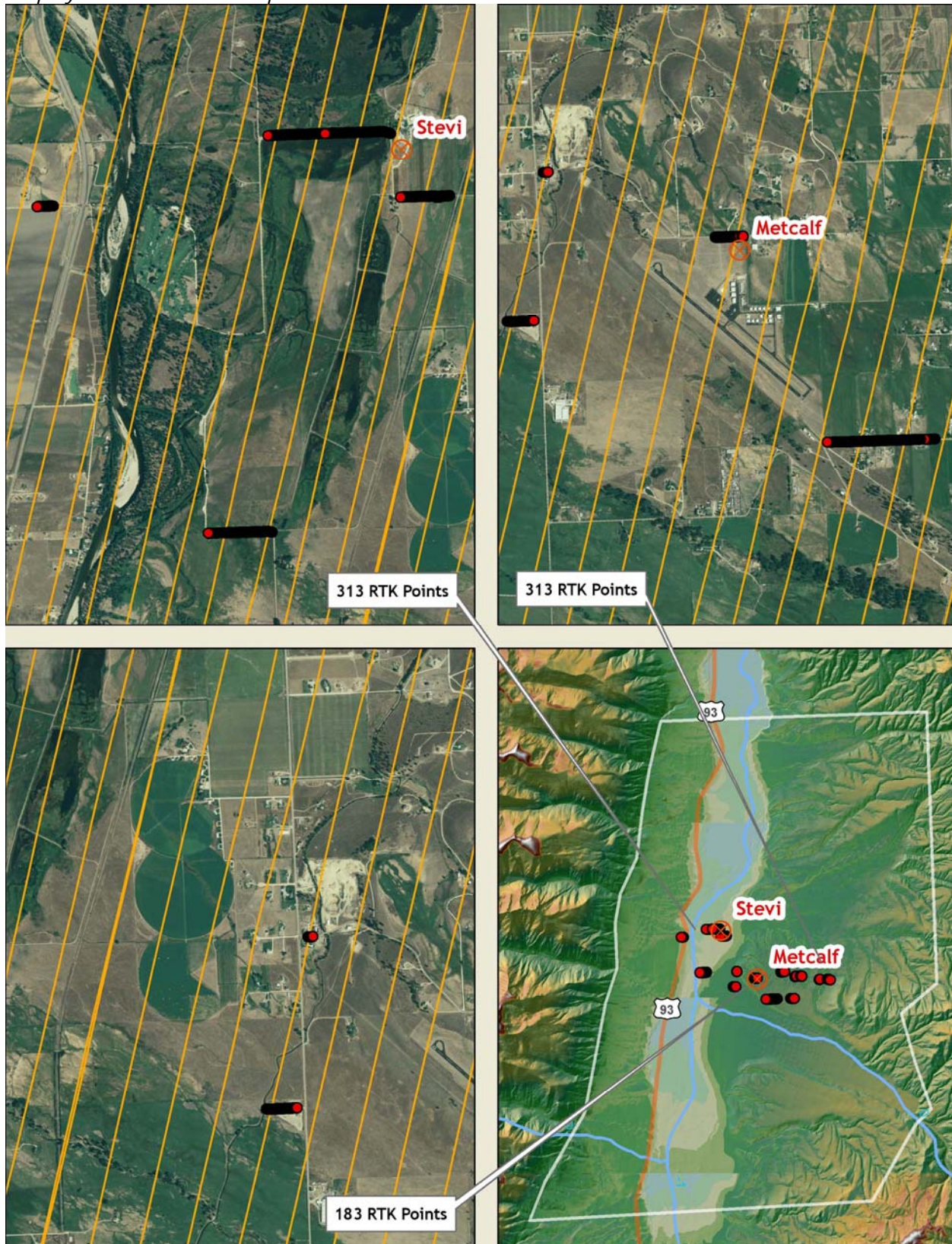
| Base Station ID | Datum NAD83 (HARN) | | GRS80 |
|-----------------|--------------------|------------------|----------------------|
| | Latitude (North) | Longitude (West) | Ellipsoid Height (m) |
| Stevi | 46 31 45.702 | 114 03 05.891 | 1070.408 |
| Metcalf | 46 33 16.002 | 114 04 35.856 | 979.135 |

Multiple differential GPS units are used in the ground based real-time kinematic (RTK) portion of the survey. To collect accurate ground surveyed points, a GPS base unit is set up over monuments to broadcast a kinematic correction to a roving GPS unit. The ground crew uses a roving unit to receive radio-relayed kinematic corrected positions from the base unit. This RTK survey allows precise location measurement ($\sigma \leq 1.5$ cm). 1024 RTK ground points were collected in the Bitterroot River Valley project area and compared to LiDAR data for accuracy assessment. **Figures 2.2 and 2.3** show base station locations and detailed RTK point locations.



² Online Positioning User Service (OPUS) is run by the National Geodetic Survey to process corrected monument positions.

Figure 2.2. GPS Base station and RTK point locations in the Bitterroot River Valley study area displayed over a NAIP Orthophoto.



3. LiDAR Data Processing

3.1 Applications and Work Flow Overview

1. Resolved kinematic corrections for aircraft position data using kinematic aircraft GPS and static ground GPS data.
Software: Waypoint GPS v.7.80, Trimble Geomatics Office v.1.62
2. Developed a smoothed best estimate of trajectory (SBET) file blending post-processed aircraft position with attitude data. Sensor head position and attitude were calculated throughout the survey. The SBET data were used extensively for laser point processing.
Software: IPAS v.1.4
3. Calculated laser point position by associating the SBET position to each laser point return time, scan angle, intensity, etc. Created raw laser point cloud data for the entire survey in .las (ASPRS v1.1) format.
Software: ALS Post Processing Software
4. Imported raw laser points into manageable blocks (less than 500 MB) to perform manual relative accuracy calibration and filtered for pits/birds. Ground points were then classified for individual flight lines (to be used for relative accuracy testing and calibration).
Software: TerraScan v.8.001
5. Using ground classified points for each flight line, the relative accuracy was tested. Automated line-to-line calibrations were then performed for system attitude parameters (pitch, roll, heading), mirror flex (scale) and GPS/IMU drift. Calibrations were performed on ground classified points from paired flight lines. Every flight line was used for relative accuracy calibration.
Software: TerraMatch v.8.001
6. Position and attitude data were imported. Resulting data were classified as ground and non-ground points. Statistical absolute accuracy was assessed via direct comparisons of ground classified points to ground RTK survey data. Data were then converted to orthometric elevations (NAVD88) by applying a Geoid03 correction.
Software: TerraScan v.8.001, TerraModeler v.8.001

3.2 Aircraft Kinematic GPS and IMU Data

LiDAR survey datasets were referenced to 1 Hz static ground GPS data collected over pre-surveyed monuments with known coordinates. While surveying, the aircraft collected 2 Hz kinematic GPS data and the inertial measurement unit (IMU) collected 200 Hz attitude data. Waypoint GPS v.7.80 was used to process the kinematic corrections for the aircraft. The static and kinematic GPS data were then post-processed after the survey to obtain an accurate GPS solution and aircraft positions. IPAS v.1.4 was used to develop a trajectory file including corrected aircraft position and attitude information. The trajectory data for the entire flight survey session were incorporated into a final smoothed best estimated trajectory (SBET) file containing accurate and continuous aircraft positions and attitudes.

3.3 Laser Point Processing

Laser point coordinates were computed using the IPAS and ALS Post Processor software suites based on independent data from the LiDAR system (pulse time, scan angle), and aircraft trajectory data (SBET). Laser point returns (first through fourth) were assigned an associated (x, y, and z) coordinate along with unique intensity values (0-255). The data were output into large LAS v. 1.1 files; each point maintaining the corresponding scan angle, return number (echo), intensity, and x, y, and z (easting, northing, and elevation) information.

These initial laser point files were too large to process. To facilitate laser point processing, bins (polygons) were created to divide the dataset into manageable sizes (< 500 MB). Flightlines and LiDAR data were then reviewed to ensure complete coverage of the study area and positional accuracy of the laser points.

Once the laser point data were imported into bins in TerraScan, a manual calibration was performed to assess the system offsets for pitch, roll, heading and mirror scale. Using a geometric relationship developed by Watershed Sciences, each of these offsets was resolved and corrected if necessary.

The LiDAR points were then filtered for noise, pits and birds by screening for absolute elevation limits, isolated points and height above ground. Each bin was then inspected for pits and birds manually, and spurious points were removed. For a bin containing approximately 7.5-9.0 million points, an average of 50-100 points were typically found to be artificially low or high. These spurious non-terrestrial laser points must be removed from the dataset. Common sources of non-terrestrial returns are clouds, birds, vapor, and haze.

Internal calibration was refined using TerraMatch. Points from overlapping lines were tested for internal consistency and final adjustments made for system misalignments (i.e., pitch, roll, heading offsets and mirror scale). Automated sensor attitude and scale corrections yielded 3-5 cm improvements in the relative accuracy. Once the system misalignments were corrected, vertical GPS drift was resolved and removed per flight line, yielding a slight improvement (<1 cm) in relative accuracy. In summary, the data must complete a robust calibration designed to reduce inconsistencies from multiple sources (i.e. sensor attitude offsets, mirror scale, GPS drift).

The TerraScan software suite is designed specifically for classifying near-ground points (Soininen 2004). The processing sequence began with removal of all points not near the earth based on geometric constraints used to evaluate multi-return points. The resulting bare earth (ground) model was visually inspected and additional ground point modeling was performed in site-specific areas (over a 50-meter radius) to improve ground detail. This was only done in areas with known ground modeling deficiencies, such as bedrock outcrops, cliffs, deeply incised stream banks, and dense vegetation. In some cases, ground point classification included known vegetation (i.e., understory, low/dense shrubs, etc.) and these points were manually reclassified as non-grounds.

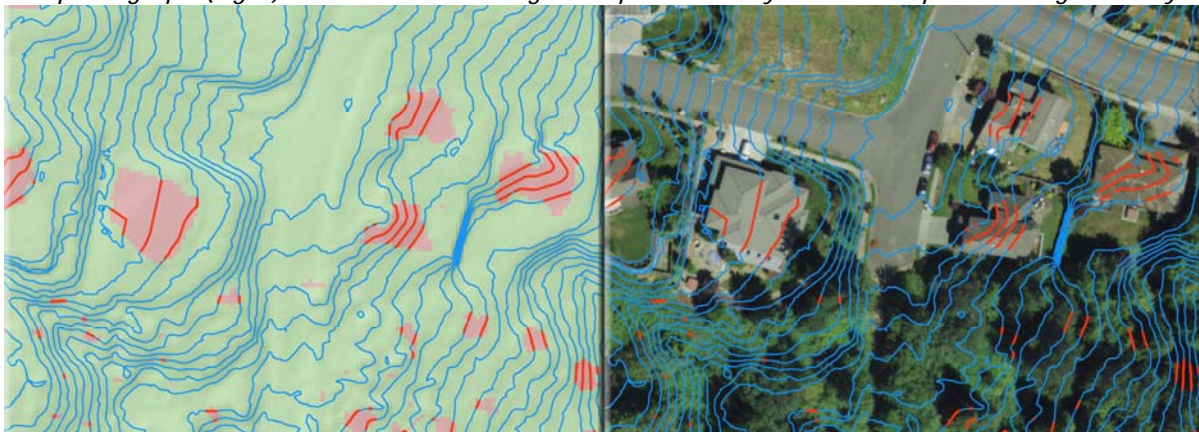
3.4 Contour Development

Contour lines were derived at a 2-foot interval from ground-classified LiDAR point data using MicroStation v. 8.01.

Ground point density rasters were created within MicroStation using a 3-foot step resolution and a 6-foot sampling radius. Areas with less than 0.02 ground-classified points per square foot (0.22 points per square meter) were considered as “sparse” and areas with higher densities were considered as “covered”. The ground point density rasters are in TIF format and have a 3-foot pixel size.

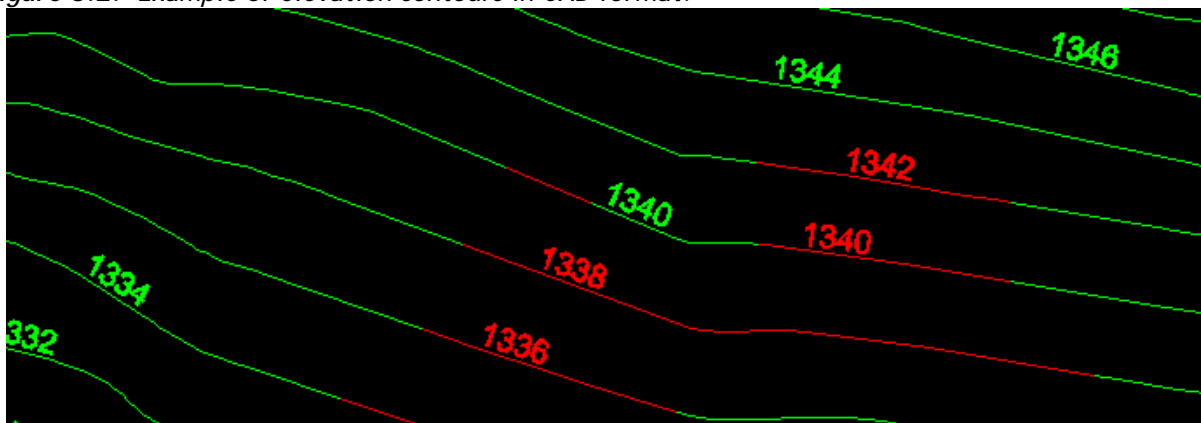
The elevation contour lines were intersected with the ground point density rasters and a confidence value was added to the contour lines. Contour lines over “sparse” areas have a low confidence, while contour lines over “covered” areas have a good confidence. Areas with low ground point density are commonly beneath buildings and bridges, in locations with dense vegetation, over water, and in other areas where the LiDAR is unable to sufficiently penetrate to the ground surface. **Figure 3.1** is an example of a ground point density raster and contour lines.

Figure 3.1. Elevation contours over LiDAR ground-classified point density raster (left) and true-color aerial photograph (right). Red indicates low ground point density and blue represents high density.



The CAD files (*.DWG) are coded to display high and low confidence contours as green and red, respectively (**Figure 3.2**). The elevation label units are feet.

Figure 3.2. Example of elevation contours in CAD format.



4. LiDAR Accuracy and Resolution

4.1 Laser Point Accuracy

Laser point absolute accuracy is largely a function of internal consistency (measured as relative accuracy) and laser noise:

- **Laser Noise:** For any given target, laser noise is the breadth of the data cloud per laser return (i.e., last, first, etc.). Lower intensity surfaces (roads, rooftops, still/calm water) experience higher laser noise. The laser noise range for this mission is approximately 0.02 meters.
- **Relative Accuracy:** Internal consistency refers to the ability to place a laser point in the same location over multiple flight lines, GPS conditions, and aircraft attitudes.
- **Absolute Accuracy:** RTK GPS measurements taken in the study areas compared to LiDAR point data.

Statements of statistical accuracy apply to fixed terrestrial surfaces only, not to free-flowing or standing water surfaces, moving automobiles, et cetera.

Table 4.1. LiDAR accuracy is a combination of several sources of error. These sources of error are cumulative. Some error sources that are biased and act in a patterned displacement can be resolved in post processing.

| Type of Error | Source | Post Processing Solution |
|---------------------------|------------------------------|---|
| GPS (Static/Kinematic) | Long Base Lines | None |
| | Poor Satellite Constellation | None |
| | Poor Antenna Visibility | Reduce Visibility Mask |
| Relative Accuracy | Poor System Calibration | Recalibrate IMU and sensor offsets/settings |
| | Inaccurate System | None |
| Laser Noise | Poor Laser Timing | None |
| | Poor Laser Reception | None |
| | Poor Laser Power | None |
| | Irregular Laser Shape | None |

4.1.1 Relative Accuracy

Relative accuracy refers to the internal consistency of the data set and is measured as the divergence between points from different flight lines within an overlapping area. Divergence is most apparent when flight lines are opposing. When the LiDAR system is well calibrated, the line to line divergence is low (<10 cm). Internal consistency is affected by system attitude offsets (pitch, roll and heading), mirror flex (scale), and GPS/IMU drift.

Operational measures taken to improve relative accuracy:

1. Low Flight Altitude: Terrain following was targeted at a flight altitude of 1000 meters above ground level (AGL). Laser horizontal errors are a function of flight altitude above ground; lower flight altitudes decrease laser noise on all surfaces.
2. Focus Laser Power at narrow beam footprint: A laser return must be received by the system above a power threshold to accurately record a measurement. The strength of the laser return is a function of laser emission power, laser footprint, flight altitude and the reflectivity of the target. While surface reflectivity cannot be controlled, laser power can be increased and low flight altitudes maintained.
3. Reduced Scan Angle: Edge-of-scan data can become inaccurate. The scan angle was reduced to a maximum of $\pm 14^\circ$ from nadir, creating a narrow swath width and greatly reducing laser shadows from trees and buildings.
4. Quality GPS: Flights took place during optimal GPS conditions (e.g., 6 or more satellites and PDOP [Position Dilution of Precision] less than 3.0). During all flight times, a dual frequency DGPS base station recording at 1-second epochs was utilized and a maximum baseline length between the aircraft and the control point was less than 18.3 km (11.4 nautical miles).
5. Ground Survey: Ground survey point accuracy (i.e., <1.5 cm RMSE) occurs during optimal PDOP ranges and targets a minimal baseline distance of 4 miles between GPS rover and base. Robust statistics are, in part, a function of sample size (n) and distribution. The ground survey collected 1024 RTK points distributed throughout multiple flight lines across the study areas.
6. 50% Side-Lap (100% Overlap): Overlapping areas were optimized for relative accuracy testing. Laser shadowing was minimized to help increase target acquisition from multiple scan angles. Ideally, with a 50% side-lap, the most nadir portion of one flight line coincides with the edge (least nadir) portion of overlapping flight lines. A minimum of 50% side-lap with terrain-followed acquisition prevents data gaps.
7. Opposing Flight Lines: All overlapping flight lines are opposing. Pitch, roll and heading errors are amplified by a factor of two relative to the adjacent flight line(s), making misalignments easier to detect and resolve.

Relative Accuracy Calibration Methodology

1. Manual System Calibration: Calibration procedures for each mission require solving geometric relationships relating measured swath-to-swath deviations to misalignments of system attitude parameters. Corrected scale, pitch, roll and heading offsets were calculated and applied to resolve misalignments. The raw divergence between lines was computed after the manual calibration and reported for the study area.
2. Automated Attitude Calibration: All data were tested and calibrated using TerraMatch automated sampling routines. Ground points were classified for each individual flight line and used for line-to-line testing. The resulting overlapping ground points (per line) in the Bitterroot River Valley study area total over 2 billion points from which to compute and refine relative accuracy. System misalignment offsets (pitch, roll and heading) and mirror scale were solved for each individual mission. Attitude misalignment offsets (and mirror scale) occurs for each individual mission. The data from each mission were then blended when imported together to form the entire area of interest.
3. Automated Z Calibration: Ground points per line were utilized to calculate the vertical divergence between lines caused by vertical GPS drift. Automated Z calibration was the final step employed for relative accuracy calibration.

Relative Accuracy Calibration Results

Relative accuracy statistics for the Bitterroot River Valley study area are based on the comparison of 96 flightlines and 2,091,022,067 points. For flightline coverage, see **Figure 2.1** in Section 2.1.

- Project average = 0.04 m
- Median relative accuracy = 0.04 m
- 1 σ relative accuracy = 0.04 m
- 2 σ relative accuracy = 0.05 m

Figure 4.1. Distribution of relative accuracies per flight line, non slope-adjusted.

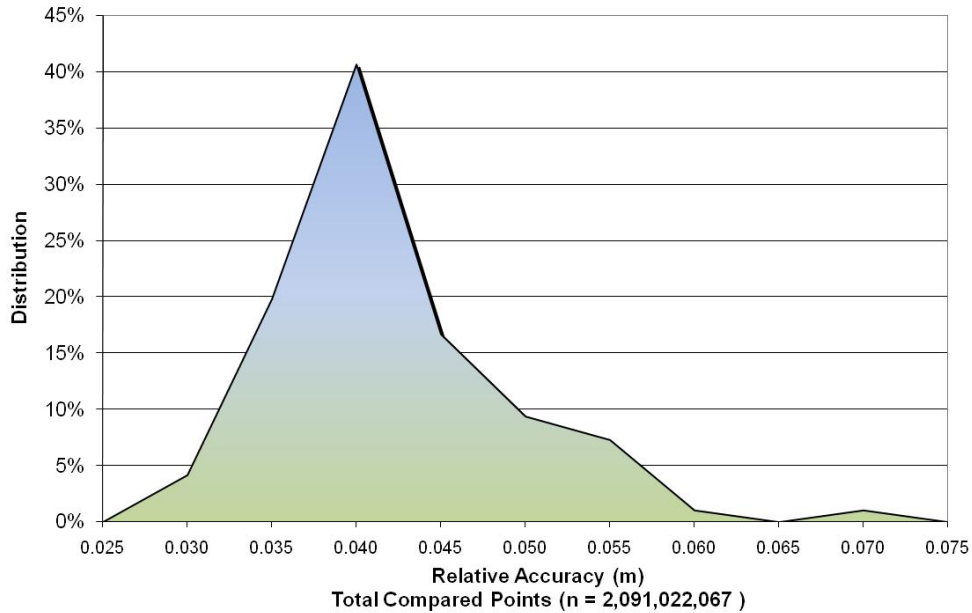
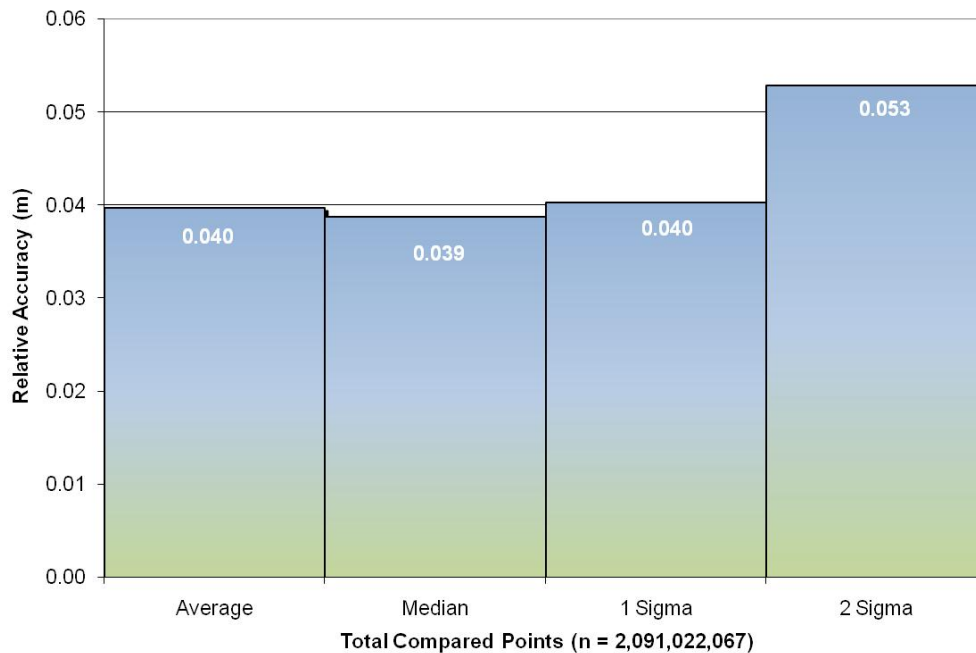


Figure 4.2. Statistical relative accuracies, non slope-adjusted.



4.1.2 Absolute Accuracy

The final quality control measure is a statistical accuracy assessment comparing known RTK ground survey points to the closest laser points.

Table 4.2. *Absolute Accuracy - Deviation between laser points and RTK survey points.*

| Sample Size (n): 1024 | |
|---------------------------------------|------------------------------|
| Root Mean Square Error (RMSE): 0.02 m | |
| Standard Deviations | Deviations |
| 1 sigma (σ): 0.02 m | Minimum Δz : -0.08 m |
| 2 sigma (σ): 0.04 m | Maximum Δz : 0.06 m |
| | Average Δz : 0.02 m |

Figure 4.3. *Absolute deviation histogram statistics.*

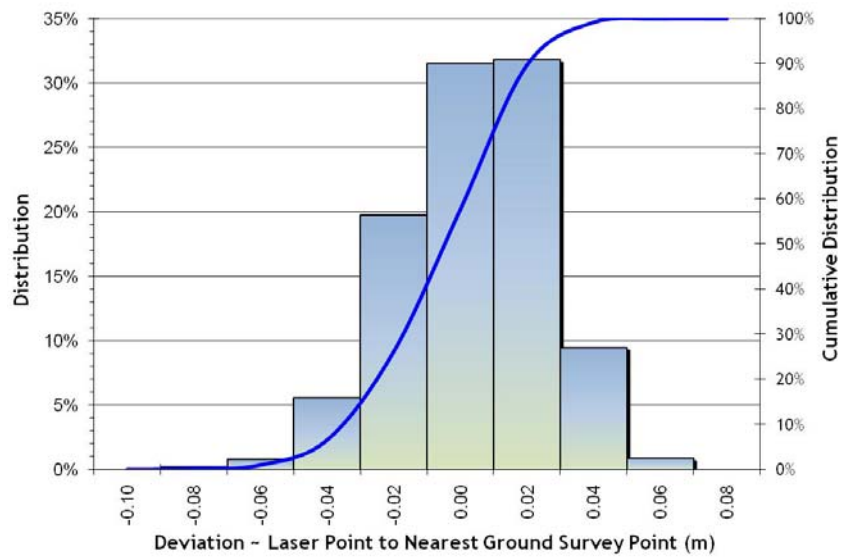
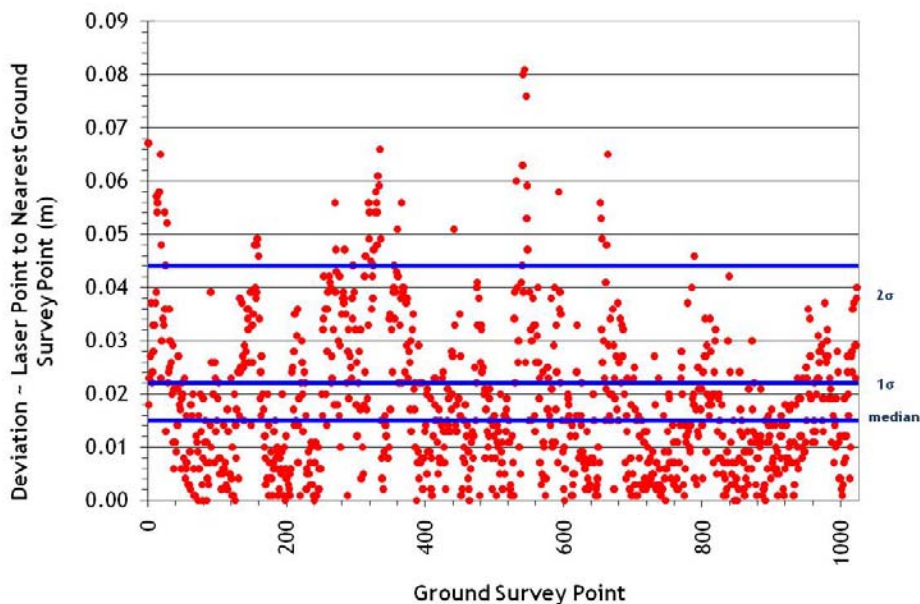


Figure 4.4. *Point absolute deviation statistics.*



4.2 Accuracy per Land Cover

Supplemental ground control points were submitted by George Marshall (licensed PLS) for compliance with FEMA standards. Individual accuracies were computed for each land-cover type to assess confidence in the LiDAR derived ground models across land-cover classes. Ground control points were accepted without review by Watershed Sciences. As such, outlier data points were not reviewed for possible exclusion from accuracy statistics. These supplemental ground control points were not used in internal quality assurance and evaluation of this LiDAR dataset. See section 4.1 (above) for internal absolute accuracy reporting. Land cover classes for FEMA specifications were described as follows:

Pavement: Urban and rural pavement surfaces, pavement edge.

Bare Earth: Open, non-vegetated surfaces, such as dirt roads, where native pulse densities are observed and there is typically one return per pulse.

Low Vegetation: Low-lying vegetation such as lawn, grass fields, alfalfa, sage.

High Vegetation: Tall vegetation such as thornbush, sage.

Shrubs: Shrub vegetation such as willows, aspen, and small saplings.

Trees: Mature trees such as cottonwood, willow, and other tree species.

Table 4.3. Summary of absolute accuracy statistics for each land cover type in the Bitterroot River Valley study area, Montana.

| Surface Type | Sample Size | Mean Dz (ft) | 1 sigma (σ) (ft) | 2 sigma (σ) (ft) | RMSE (ft) |
|--------------|-------------|--------------|---------------------------|---------------------------|-----------|
| Pavement | 32 | 0.09 | 0.12 | 0.29 | 0.14 |
| Bare Earth | 77 | 0.07 | 0.14 | 0.28 | 0.13 |
| Low Veg | 33 | 0.23 | 0.31 | 0.50 | 0.19 |
| High Veg | 33 | 0.32 | 0.35 | 0.68 | 0.22 |
| Shrubs | 20 | 0.45 | 0.44 | 1.08 | 0.33 |
| Trees | 75 | 0.16 | 0.24 | 0.54 | 0.28 |

Shrub land class accuracy statistics may be influenced by small n (20 observations) and the presence of outlier data points. Outlier points may be explained by GPS instrument occlusion (shading) resulting in poor GPS resolution as well as LiDAR ground resolution failure at the point of ground survey (i.e. the ground survey point coincides with an area unresolved in the LiDAR data where the modeled terrain is simplified through interpolation).

4.3 Data Density/Resolution

Some types of surfaces (i.e. dense vegetation or water) may return fewer pulses than originally emitted by the laser. Delivered density may therefore be less than the native density and vary according to distributions of terrain, land cover, and water bodies.

4.3.1 First Return Laser Pulses per Square Meter

The average density of first return pulses for the Bitterroot River Valley study area data is 6 points/m².

Figure 4.5. Histogram of first return laser point density.

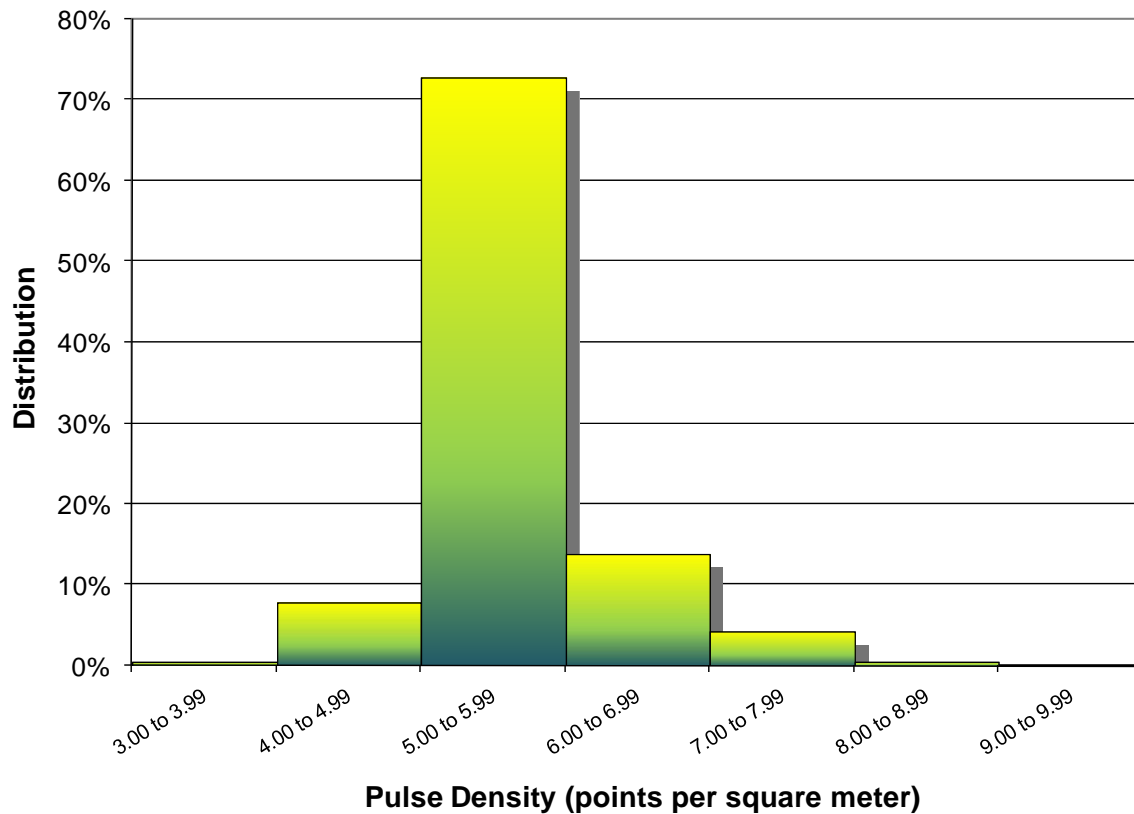
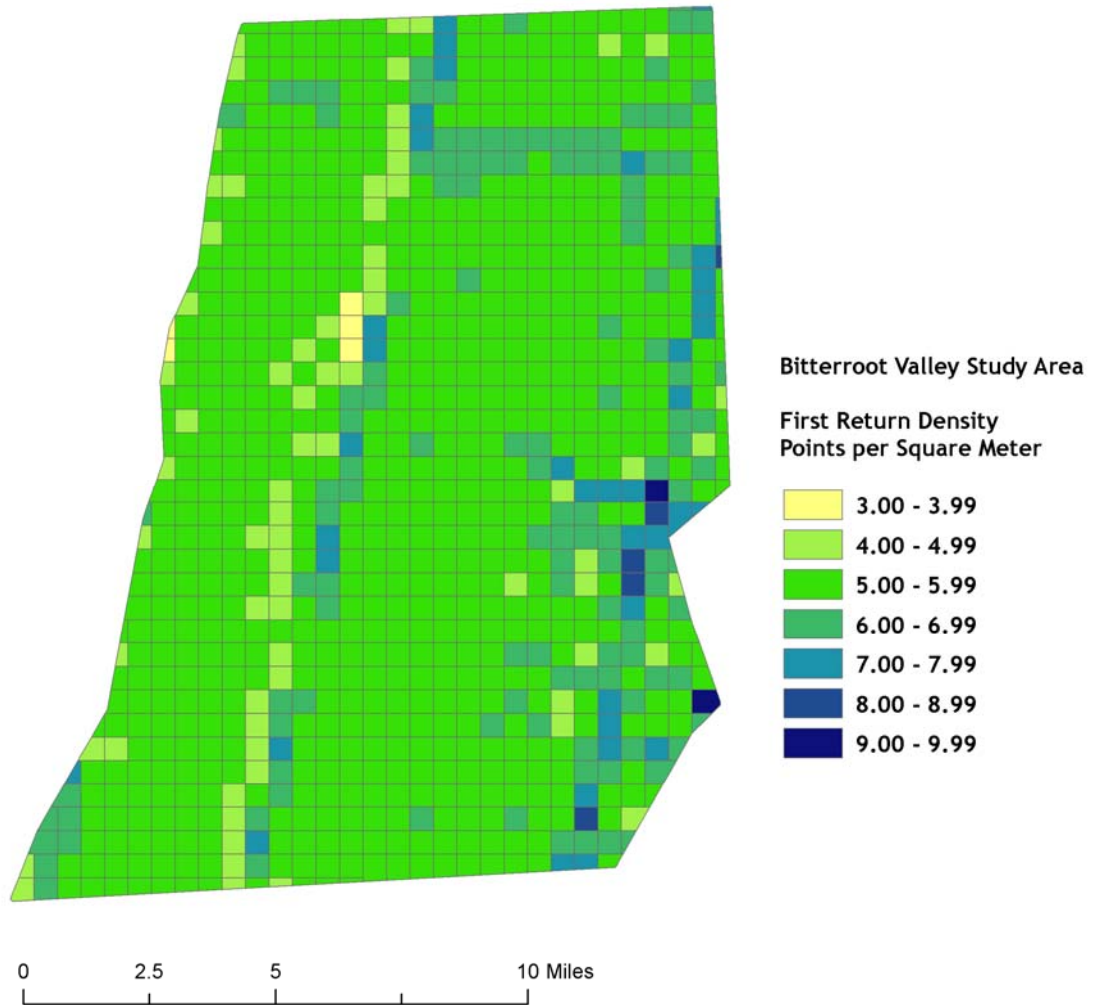


Figure 4.6. First return laser point data density by processing bin.



4.3.2 Ground Classified Points per Square Meter

Ground classifications are derived from ground surface modeling. Supervised classifications were performed by reseeded where it is determined that the ground model has failed, usually under dense vegetation, at breaks in terrain, or at bin boundaries.

The average ground point density for the Bitterroot River Valley data is 2 points/m².

Figure 4.7. Histogram of ground-classified data density.

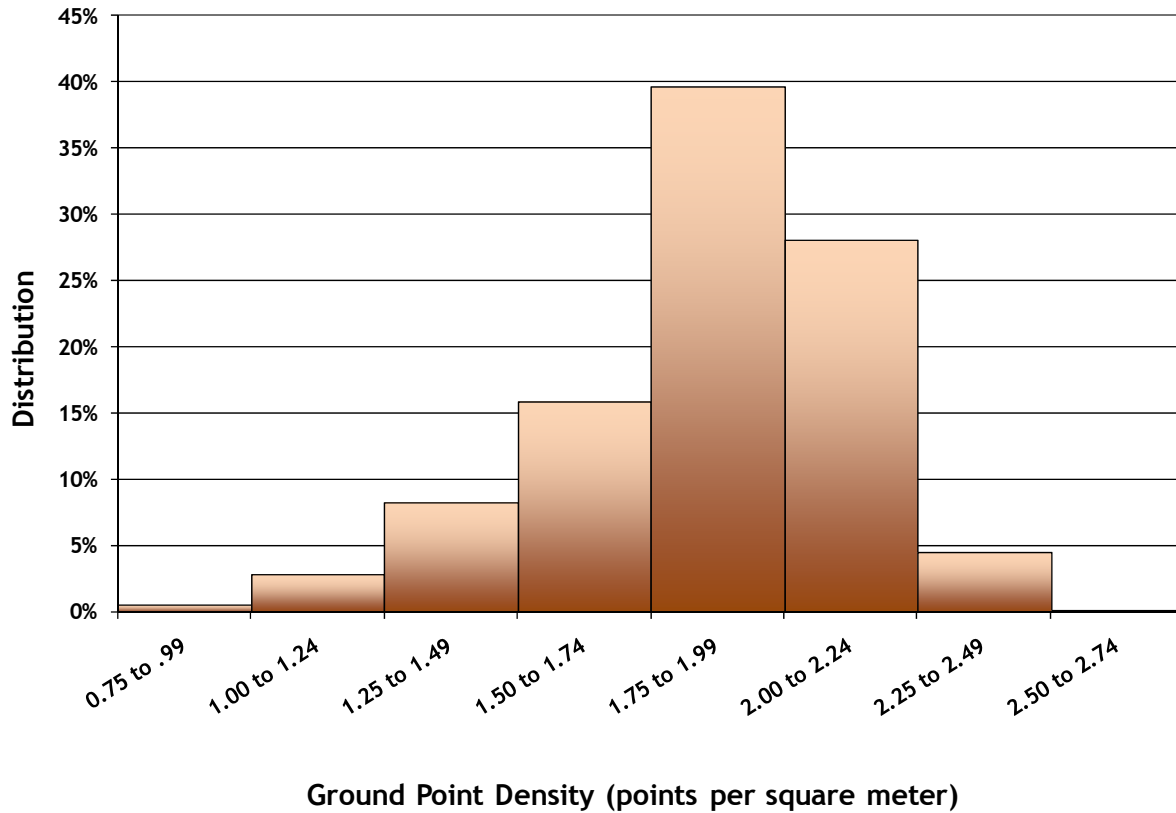
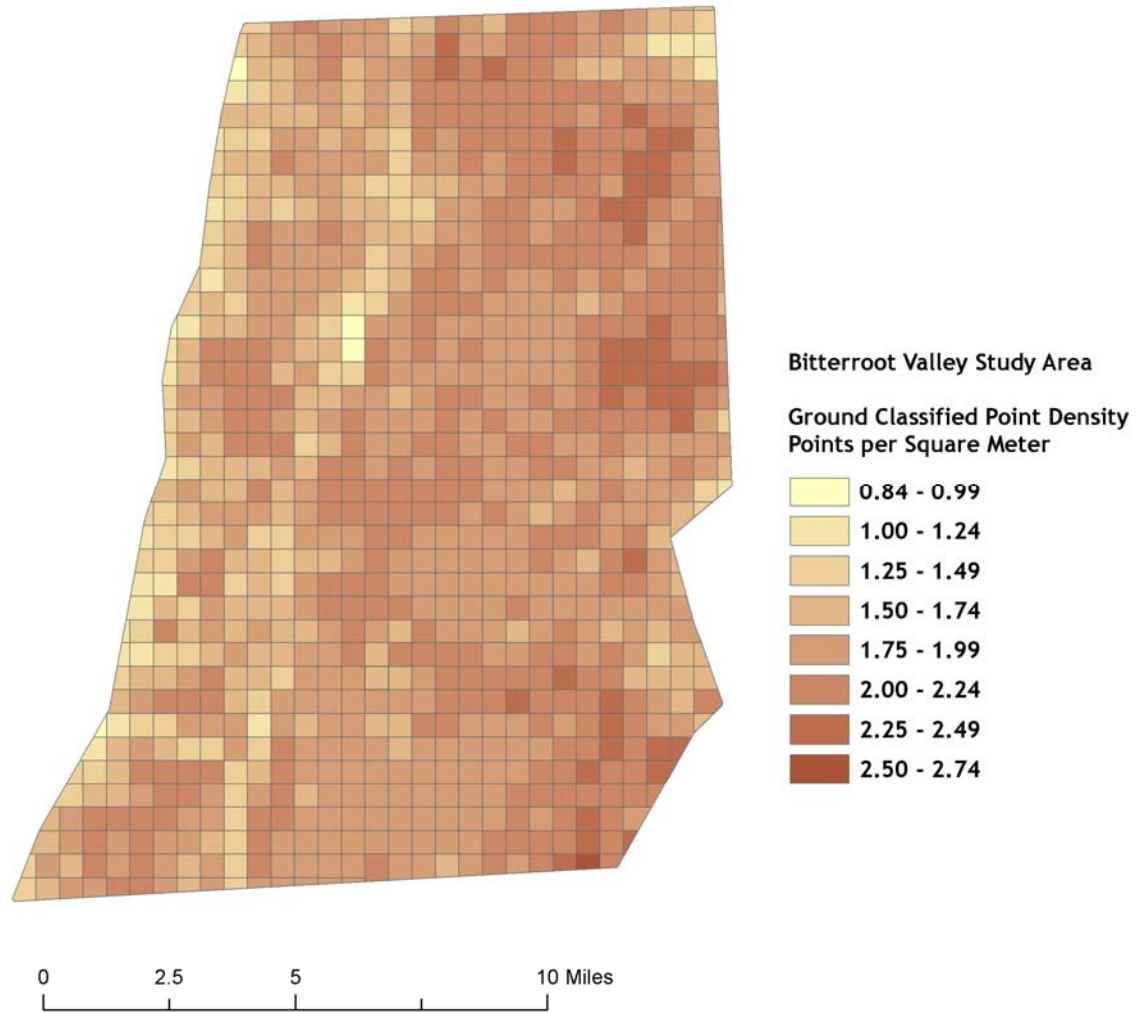


Figure 4.8. Ground-classified point data density by processing bin.



5. Data Specifications

| | Targeted | Achieved |
|----------------------------------|--------------------------|-------------------------|
| Resolution: | >6 points/m ² | 6 points/m ² |
| Vertical Accuracy (1 σ): | <18.5 cm | 2 cm |

6. Projection/Datum and Units

The data were processed as ellipsoidal elevations and required a Geoid transformation to be converted into orthometric elevations (NAVD88). In TerraScan, the NGS published Geoid03 model is applied to each point. The data were processed using meters in the Universal Transverse Mercator (UTM) Zone 11 and NAD83 (CORS96)/NAVD88 datum.

| | | |
|-------|-------------|---|
| | Projection: | Montana State Plane |
| Datum | Vertical: | NAVD88/Geoid03 |
| | Horizontal: | NAD83 |
| | Units: | Point and Raster datasets: Meters Contour datasets: US Survey Feet |

7. Deliverables

7.1 Point Data

- All return point cloud delineated by processing bin (750 m x 750 m) in Las v.1.1 format.

7.2 Raster Data

- 1-meter resolution ground surface model in ESRI grid format
- 1-meter resolution highest hit model in ESRI grid format
- ½-meter resolution surface intensity images in GeoTIFF format
- 3-foot resolution ground density raster (corresponding to contour uncertainty information).

7.3 Vector Data

- ½-meter contour data in AutoCad .dwg and ESRI .shp format

7.4 Data Report

- Report containing introduction, methodology, accuracy assessments, and sample imagery
 - Word Format (.doc)
 - PDF Format (.pdf)

8. Selected Images

Figure 8.1. Plan view of confluence between Wheelbarrow and Grayhorse Creeks. Top image is derived from bare earth LiDAR; center image from highest hit LiDAR; bottom image is a NAIP orthophoto.

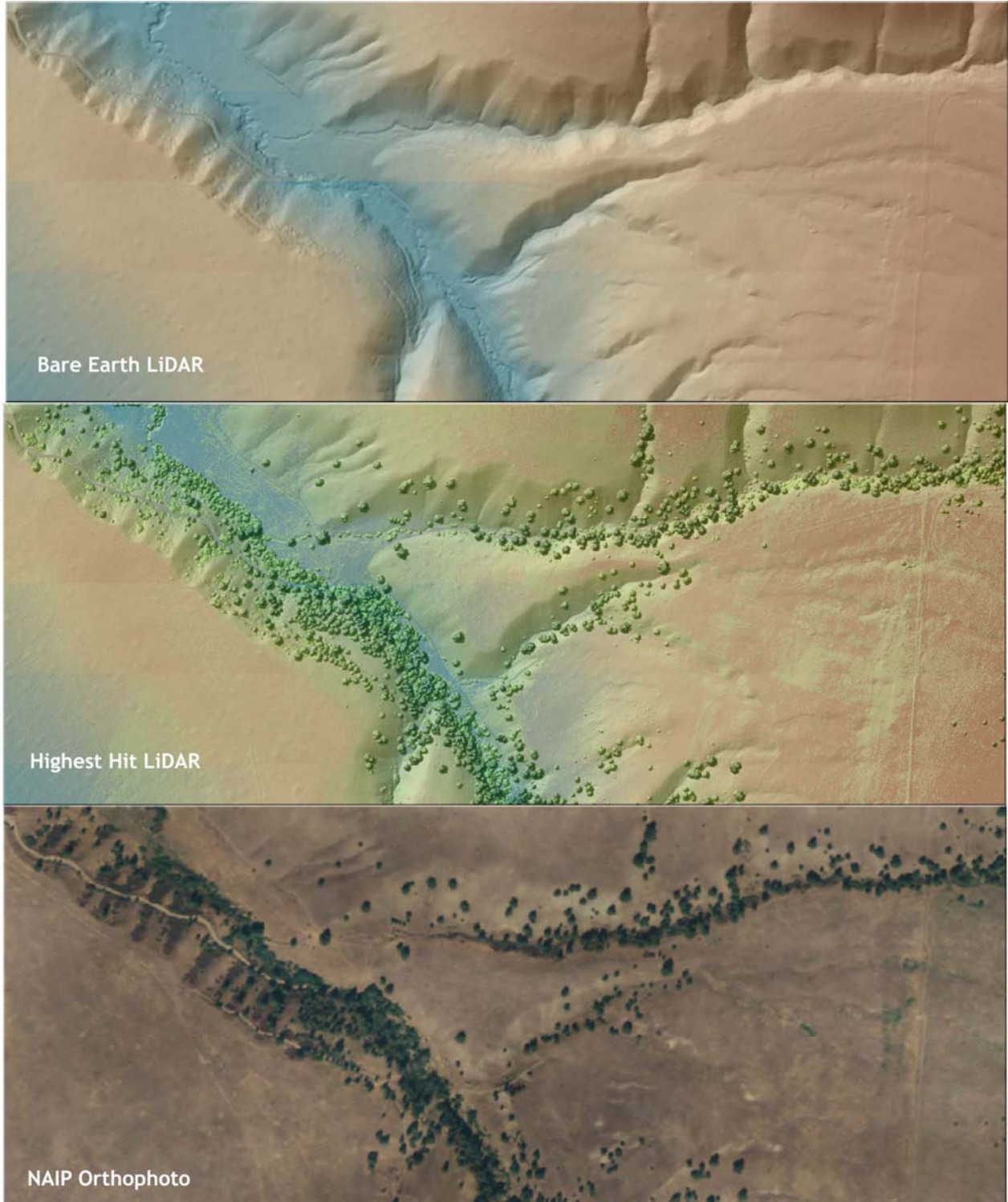


Figure 8.2 Plan view of Bitterroot floodplain with Spring Creek and Threemile Creek. Top image is bare earth LiDAR; middle image is highest hit LiDAR; lower image is NAIP orthophoto.



Figure 8.3. View downstream to northeast over Grayhorse Creek. Top image derived from highest hit LiDAR, lower image derived from bare earth LiDAR.

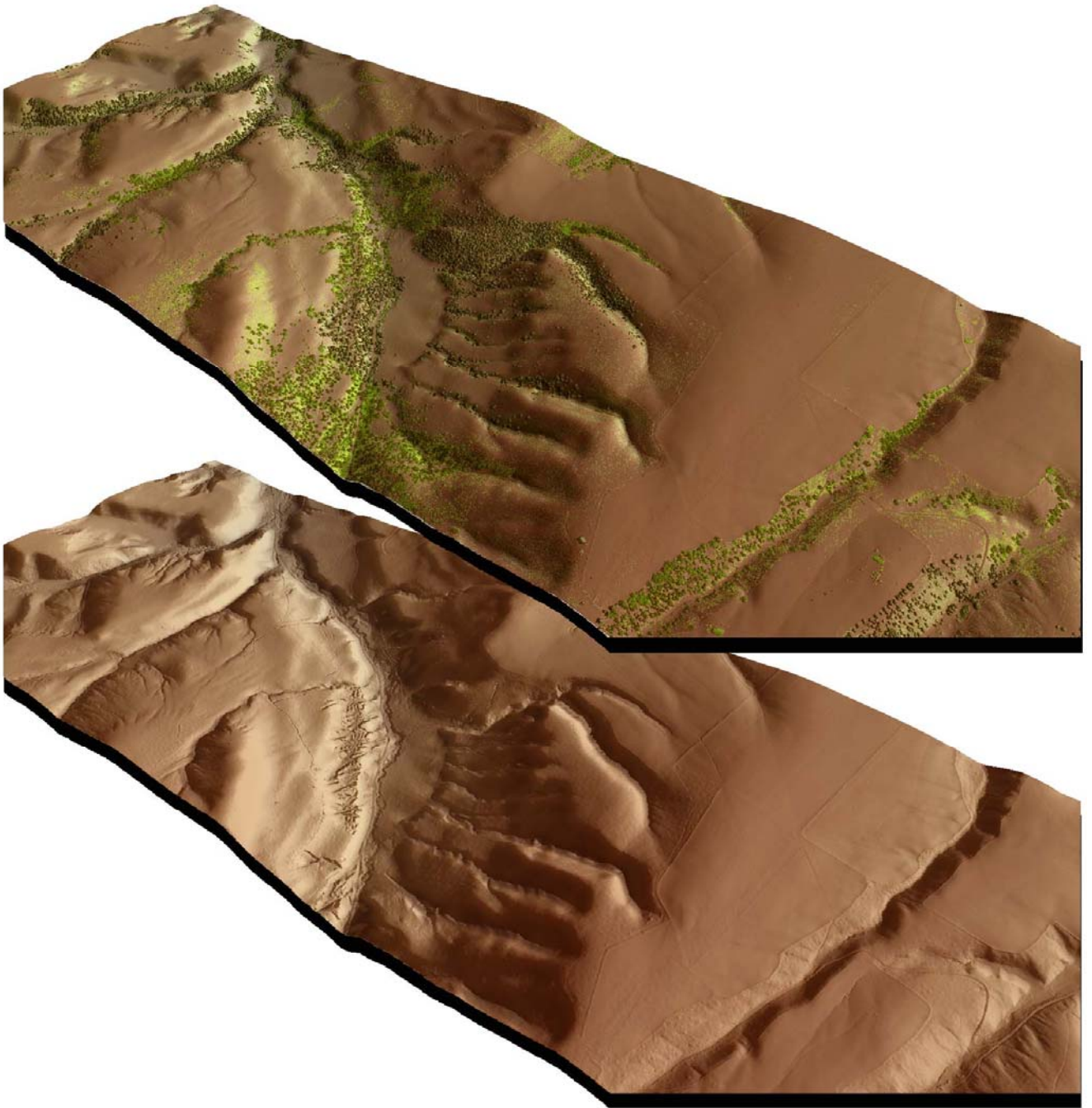
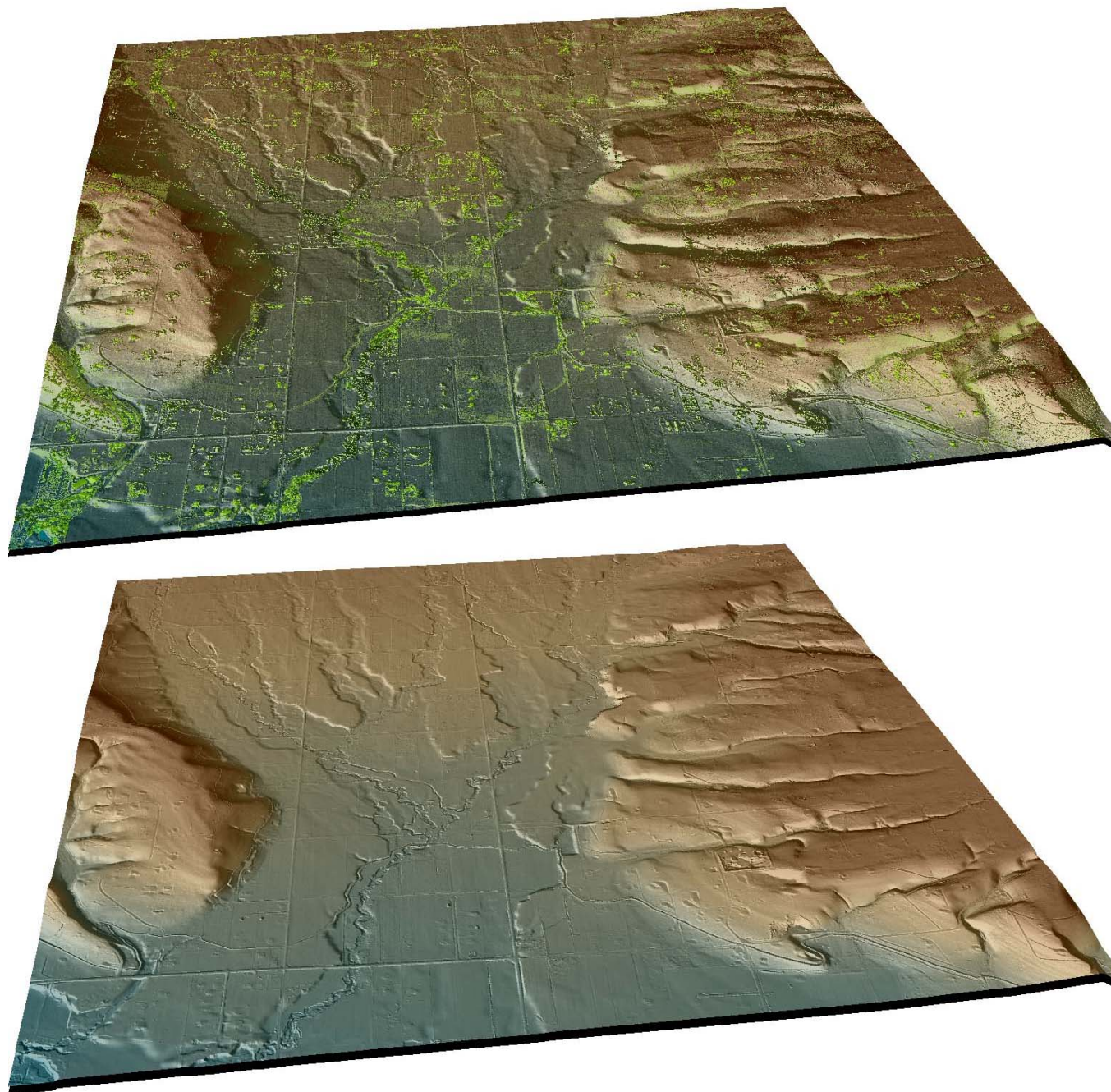


Figure 8.4. View eastward up Threemile Creek watershed. Top image derived from highest hit LiDAR, lower image derived from bare earth LiDAR.



9. Glossary

1-sigma (σ) Absolute Deviation: Value for which the data are within one standard deviation (approximately 68th percentile) of a normally distributed data set.

2-sigma (σ) Absolute Deviation: Value for which the data are within two standard deviations (approximately 95th percentile) of a normally distributed data set.

Root Mean Square Error (RMSE): A statistic used to approximate the difference between real-world points and the LiDAR points. It is calculated by squaring all the values, then taking the average of the squares and taking the square root of the average.

Pulse Rate (PR): The rate at which laser pulses are emitted from the sensor; typically measured as thousands of pulses per second (kHz).

Pulse Returns: For every laser pulse emitted, the Leica ALS 50 Phase II system can record *up to four* wave forms reflected back to the sensor. Portions of the wave form that return earliest are the highest element in multi-tiered surfaces such as vegetation. Portions of the wave form that return last are the lowest element in multi-tiered surfaces.

Accuracy: The statistical comparison between known (surveyed) points and laser points. Typically measured as the standard deviation (σ) and root mean square error (RMSE).

Intensity Values: The peak power ratio of the laser return to the emitted laser. It is a function of surface reflectivity.

Data Density: A common measure of LiDAR resolution, measured as points per square meter.

Spot Spacing: Also a measure of LiDAR resolution, measured as the average distance between laser points.

Nadir: A single point or locus of points on the surface of the earth directly below a sensor as it progresses along its flight line.

Scan Angle: The angle from nadir to the edge of the scan, measured in degrees. Laser point accuracy typically decreases as scan angles increase.

Overlap: The area shared between flight lines, typically measured in percents; 100% overlap is essential to ensure complete coverage and reduce laser shadows.

DTM / DEM: These often-interchanged terms refer to models made from laser points. The digital elevation model (DEM) refers to all surfaces, including bare ground and vegetation, while the digital terrain model (DTM) refers only to those points classified as ground.

Real-Time Kinematic (RTK) Survey: GPS surveying is conducted with a GPS base station deployed over a known monument with a radio connection to a GPS rover. Both the base station and rover receive differential GPS data and the baseline correction is solved between the two. This type of ground survey is accurate to 1.5 cm or less.

10. Citations

Soininen, A. 2004. TerraScan User's Guide. TerraSolid.